Journal of Dermatological Science 60 (2010) 95–104

Contents lists available at ScienceDirect

Journal of Dermatological Science

journal homepage: www.elsevier.com/jds

Epiplakin accelerates the lateral organization of keratin filaments during wound healing

Kazushi Ishikawa [a,b], Hideaki Sumiyoshi [b], Noritaka Matsuo [b], Naoko Takeo [a], Mizuki Goto [a], Osamu Okamoto [a], Shuji Tatsukawa [c], Hirokazu Kitamura [c], Yoshihisa Fujikura [c], Hidekatsu Yoshioka [b], Sakuhei Fujiwara [a,*]

[a] Department of Dermatology, Faculty of Medicine, Oita University, Hasama-machi, Oita, Japan
[b] Department of Matrix Biology, Faculty of Medicine, Oita University, Hasama-machi, Oita, Japan
[c] Department of Molecular Anatomy, Faculty of Medicine, Oita University, Hasama-machi, Oita, Japan

ARTICLE INFO

Article history:
Received 7 March 2010
Received in revised form 3 August 2010
Accepted 25 August 2010

Keywords:
Bullous pemphigoid
Epiplakin
Keratin
Keratinocyte
Wound healing

ABSTRACT

Background: Epiplakin (EPPK) belongs to the plakin family of cytolinker proteins and, resembling other members of the plakin family such as BPAG1 (an autoantigen of bullous pemphigoid) and plectin, EPPK has plakin repeat domains (PRDs) that bind to intermediate filaments. Elimination of EPPK by gene targeting in mice resulted in the acceleration of keratinocyte migration during wound healing. EPPK is expressed in proliferating keratinocytes at wound edges and, in view of its putative function in binding to keratin, we postulated that the keratin network in EPPK-null ($EPPK^{-/-}$) mice might be disrupted during wound healing.
Objective: To examine this hypothesis and to determine the precise localization of EPPK in relation to keratin filaments, we compared the non-wounded and wounded epidermis of wild-type and $EPPK^{-/-}$ mice.
Methods: Non-wounded epidermis and wounded epidermis from wild-type and $EPPK^{-/-}$ mice were examined by immunofluorescence staining and electron microscopy before and after double immunostaining.
Results: EPPK was colocalized with keratin 17 (K17) more extensively than with other keratins examined in wounded epidermis. The expression of K5, K10, K6, and K17 was the same in $EPPK^{-/-}$ mice after wounding as in normal mice, but diameters of keratin filaments were reduced in $EPPK^{-/-}$ keratinocytes. Electron microscopy after immunostaining revealed that EPPK colocalized with K5, K10 and K6 after wounding in wild-type mice.
Conclusion: Our data indicate that EPPK accelerates keratin bundling in proliferating keratinocytes during wound healing and suggest that EPPK might contribute to reinforcement of keratin networks under mechanical stress.

1. Introduction

Epiplakin (EPPK) belongs to the plakin family of cytolinker proteins. It is expressed mainly in the upper layers of the epidermis and it was identified as an antigen in autoimmune blistering disease [1]. EPPK is a plakin but has some unusual features. Human EPPK has 13 domains and mouse EPPK has 16 domains that are homologous to the B domain, one of the plakin repeat domains (PRDs) found in the carboxy-terminal region of desmoplakin. These domains are distributed along the entire amino acid sequences of human and murine EPPK with relatively uniform spacing comprised of so-called linker regions [1,2]. As in the case of other members of the plakin family, namely, BPAG1 (an autoantigen of bullous pemphigoid) and plectin, experiments *in vitro* have demonstrated that the PRDs and/or linker regions of EPPK bind to intermediate filaments [3–5].

To examine the functions of EPPK, we generated $EPPK^{-/-}$ mice. Under normal conditions, there were no detectable differences between wild-type and $EPPK^{-/-}$ mice. However, wounds on the backs of $EPPK^{-/-}$ mice closed more rapidly than those on the backs of wild-type mice and of heterozygous mice. At wound edges in wild-type mice, EPPK was expressed in proliferating keratinocytes; in $EPPK^{-/-}$ mice, there seemed to be fewer proliferating keratinocytes [6].

We postulated that EPPK might be linked, functionally, to keratin networks during wound healing and, in the present study, we examined the relationship between the expression and

* Corresponding author. Tel.: +81 97 586 5882; fax: +81 97 586 5889.
E-mail address: fujiwara@oita-u.ac.jp (S. Fujiwara).

0923-1811/$36.00
doi:10.1016/j.jdermsci.2010.08.011

localization of EPPK on the other hand and the formation and characteristics of keratin networks during wound healing.

2. Materials and methods

2.1. Expression of glutathione S-transferase-tagged (GST-tagged) fusion proteins and preparation of polyclonal antibodies

Glutathione S-transferase-EPPK (GST-EPPK) fusion protein, which included the linker region between the 15th and 16th B domains of mouse EPPK [6], and GST-keratin 5 (GST-K5) fusion protein, which included the carboxy-terminal region of mouse K5 were expressed in *E. coli*. The purified recombinant proteins were mixed, separately, with an equal volume of Freund's complete adjuvant (Difco, Detroit, MI, USA) and injected subcutaneously into rabbits (EPPK) or rats (EPPK and K5). The animals were given two subsequent booster injections plus Freund's incomplete adjuvant (Difco). Rats were bled 1 week after the second booster injection. Affinity purification of antibodies was performed by coupling the GST-fusion proteins to CNBr-activated Sepharose (GE Healthcare UK Ltd., Buckinghamshire, England) according to the instructions from the manufacture. Rat sera prepared from the final bleeds were incubated with each Sepharose-fusion protein complex for 24 h at 4 °C and then the complex was washed with phosphate-buffered saline (PBS). Then bound antibodies were eluted with 200 mM glycine–HCl (pH 2.3), which was then neutralized immediately with 1 M Tris–HCl (pH 7.4). We confirmed that the antibodies, which we used in this study, were specific against EPPK using western blotting.

2.2. Generation of model wounds

Mice were anesthetized with an intraperitoneal injection of ketamine and xylazine, as described elsewhere [6]. The dorsal surface was shaved, and a disposable skin-punch biopsy tool of 0.6 cm in diameter (Health Link, Jacksonville, FL, USA) was used to create a full-thickness excision wound that extended to the fascia, as described previously [6].

2.3. Histology and immunohistochemistry

Mice were perfused intracardially with about 100 ml of PBS per mouse, which was followed by about 200 ml of 4% paraformaldehyde per mouse. Skin was fixed in 4% paraformaldehydes, washed in PBS (pH 7.4) and then dehydrated by passage through an ethanol series (50%, 70%, 80%, 95% and twice× 100%). After embedding in paraffin block, 6-μm sections were cut on slides, deparaffinized and stained with hematoxylin and eosin.

For immunohistochemical staining, skin was fixed and sectioned as described above. All sections were blocked with 3% (w/v) bovine serum albumin (BSA) for 30 min. Sections were incubated with primary antibodies for 1 h at room temperature, rinsed with PBS, and then incubated for 2 h with appropriately modified second antibodies as described below.

For double-immunofluorescence staining, primary antibodies were applied as cocktails prepared with two of the following three antibodies: (1) polyclonal antibodies raised in rats against mouse K5 (diluted 1:50); (2) monoclonal antibodies raised in mouse against mouse K6 (diluted 1:1000, Abcam Ltd., Cambridge, United Kingdom); (3) polyclonal antibodies raised in rabbits against mouse K10 (diluted 1:50, Covance, Berkeley, CA, USA); (4) polyclonal antibodies raised in rabbits against mouse K17 (diluted 1:1000, ASB, San Diego, CA, USA) and (5) polyclonal antibodies raised in rabbits or rats against mouse EPPK (diluted 1:50). Cocktails containing primary antibodies were prepared in PBS with 1% (w/v) BSA. Sections that had been blocked with 3% (w/v) BSA for 1 h were incubated with primary antibodies for 1 h at 4 °C. After washing in PBS, sections were incubated for 2 h at room temperature, in darkness with two of the following four reagents:(1) Alexa Fluor 488-conjugated antibodies raised in goat against mouse IgG (diluted 1:1000; Molecular Probes, Eugene, OR, USA); (2) Alexa Fluor 488-conjugated antibodies raised in goat against rabbit IgG (diluted 1:1000; Molecular Probes); (3) Alexa Fluor 568-conjugated antibodies raised in goat against rat IgG (diluted 1:1000; Molecular Probes); and (4) Alexa Fluor 594-conjugated antibodies raised in goat against mouse IgG (diluted 1:1000; Molecular Probes). Immunofluorescence-labelled sections were rinsed in PBS and mounted on glass slides with Vectashield® anti-fade solution (Vector Laboratories, Burlingame, CA, USA) and coverslips. Sections were analyzed with a confocal laser scanning microscope (LSM5 PASCAL, Carl Zeiss, Jena, Germany). For generation and analysis of composite images, we used Adobe Photoshop (version 7.0; Adobe Systems, San Jose, CA, USA).

2.4. Electron microscopy

Mice were perfused intracardially with about 100 ml of PBS per mouse, which was followed by about 200 ml of 4% paraformaldehyde per mouse. Skin was fixed in 2% glutaraldehyde plus 2% formaldehyde in cacodylate buffer (0.05 M cacodylate) for 2 h. These samples were rinsed in cacodylate buffer, postfixed in 2% osmium tetroxide in cacodylate buffer containing 0.5% of potassium ferrocyanide for 2 h and rinsed again in this buffer. Then, samples were dehydrated in a graded ethanol series, as described above, embedded in epoxy-resin (LX112; Ladd Research, Burlington, VT, USA), and cut into ultrathin sections (50–70 nm thickness). Sections were placed on copper grids, counterstained with uranyl acetate and lead citrate, and examined under a transmission electron microscope (JEM-1200EX II, JEOL, Tokyo, Japan) operated at 80 kV. Diameters of keratin filaments were measured on electron micrographs of samples from six wild-type and six $EPPK^{-/-}$ mice; 250 filaments were measured in each case.

2.5. Double immunostaining and subsequent electron microscopy

Mice were perfused intracardially as described above and skin was fixed in 4% paraformaldehyde for 2 h, and then dehydrated in a graded ethanol series, as described above, and embedded in LR White resin (London Resin, Basingstoke, UK). Ultrathin sections (100–120 nm thickness) were cut with an ultramicrotome and mounted on gold grids. Sections were incubated with the primary antibodies described above plus 1% BSA for 1 h. After rinsing in PBS, sections were incubated with EM antibodies raised in goat against rat IgG: 15 nm Gold, EM antibodies raised in goat against rabbit IgG: 5 nm Gold, and EM antibodies raised in goat against mouse IgG: 5 nm Gold (BB International, Cardiff, UK), and then rinsed with PBS and with distilled water. The immunolabeled sections were stained with a saturated solution of uranyl acetate containing lead citrate in distilled water. After the sections had been washed in distilled water and dried, they were examined under an electron microscope (JEM-1200 EX II) at an accelerating voltage of 60 kV.

2.6. Statistical analysis

The statistical significance of differences was determined by student's *t*-test.

3. Results

3.1. EPPK was colocalized with keratin 10 (K10) in unwounded wild-type epidermis

In skin from wild-type mice, confocal laser scanning microscopy, after double immunostaining with antibodies against keratin 5

(K5), against keratin 10 (K10) and against EPPK, revealed that EPPK was colocalized mainly with K10 and not with K5 in the cytoplasm of cells in the suprabasal layer of the epidermis (Fig. 1A, B, C, E, F and G). In EPPK$^{-/-}$ mice, K5 and K10 were localized similarly to those in wild-type mice (Fig. 1D and H). Electron microscopic analysis of the keratinocytes of wild-type and EPPK$^{-/-}$ mice failed to reveal any differences, as described previously [6]. Immunostaining and electron microscopy revealed EPPK in the cytoplasm of cells in the suprabasal layer, adjacent to keratin fibers that had been immunostained with K10-specific antibodies in the normal epidermis of wild-type mice (Fig. 1I). No EPPK was detected in EPPK$^{-/-}$ mice (data not shown).

3.2. EPPK was expressed together with K5, K6, K10 and K17 during wound healing in wild-type skin

We monitored the expression of keratins using antibodies against K5, K10, K6 and K17 at the proliferating edge and leading edge of wounds. In wild-type mice, 4 days after wounding, expression of K5 was detected not only in the basal layer but also in the thickened epidermis of the wound's edge (Fig. 2A). K10 was also expressed in almost all cells in the suprabasal layer at the wounds edge (Fig. 2E). K6 was expressed at almost the same sites as K10 (Fig. 2I). K17 was expressed in the suprabasal region of the proliferating epidermis (Fig. 2M). EPPK was expressed in the suprabasal region of the proliferating epidermis with the exception of the tip of the leading edge (Fig. 2B, F, J and N). Although EPPK coexpressed with K5, K10 and K6 in larger epidermal cells at the wound's edge (Fig. 2C, G and K), EPPK was colocalized predominantly with K17 in the keratinocytes at wound edge (Fig. 2O).

In EPPK$^{-/-}$ mice, the pattern of expression of K5 was almost the same as in wild-type mice, and K5 was expressed in the proliferating keratinocytes at the wound's edge (Fig. 2D). The patterns of expression of K10, K6 and K17 were also similar to those in wild-type mice (Fig. 2H, L and P). The intercellular spaces in the wounded epidermis of EPPK$^{-/-}$ mice were more irregular than those in wild-type mice (Fig. 2G and H, inset)

3.3. EPPK and the absence of EPPK influenced the characteristics of keratins during wound healing

To characterize the cytoarchitectural changes in keratinocytes in EPPK$^{-/-}$ mice, we examined skin from both wild-type and EPPK$^{-/-}$ mice by transmission electron microscopy.

Four days after wounding, the cytoplasm of keratinocytes of wild-type mice near the basal and in the suprabasal layer

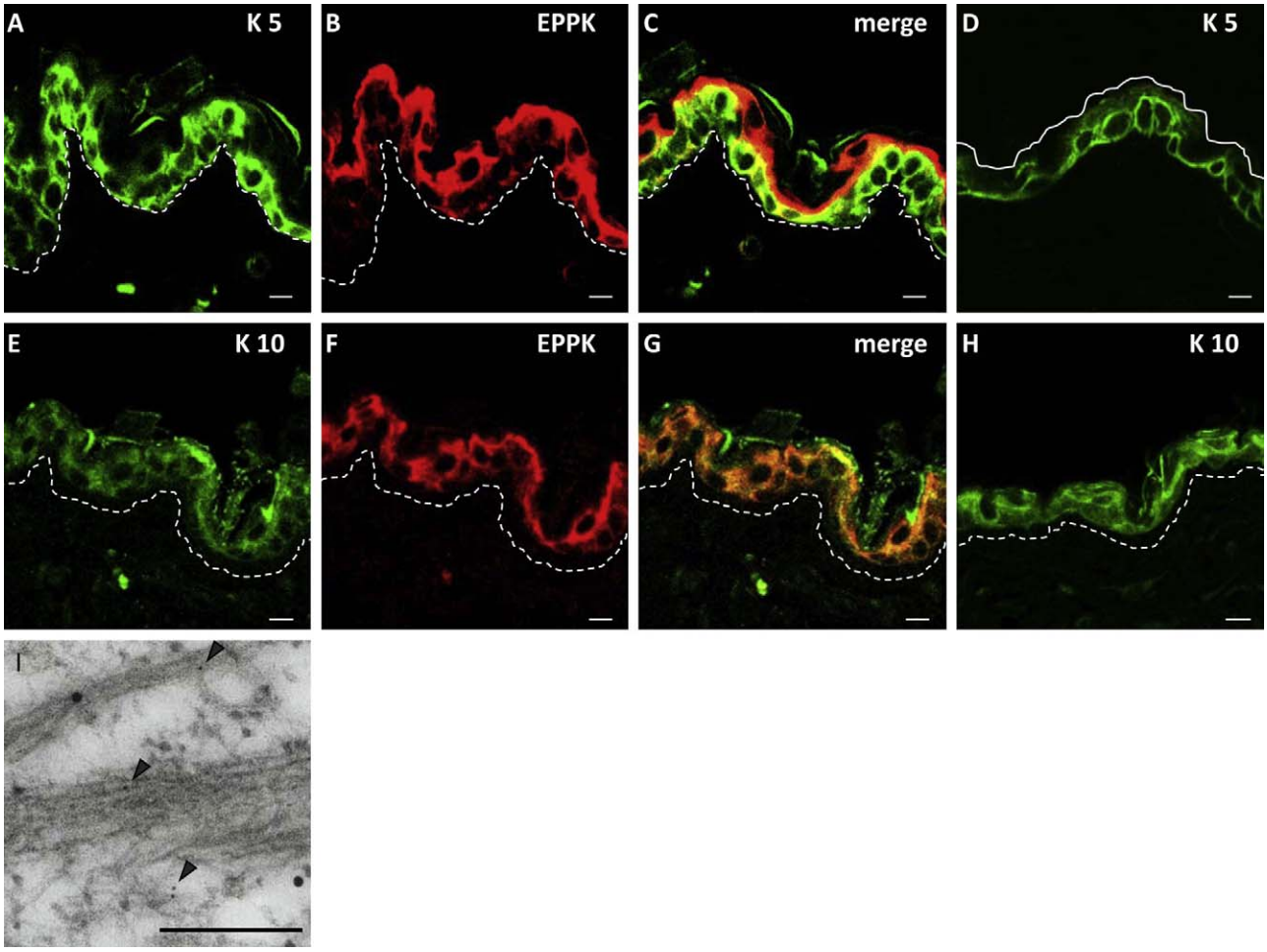

Fig. 1. Analysis by confocal laser scanning microscopy and electron microscopy after immunostaining of the unwounded dorsal skin of wild-type (A–C, E–G and I) and EPPK$^{-/-}$ (D and H) mice. K5 (A) and K10 (E) (both visualized in green) were expressed in the basal layers and suprabasal layers, respectively, of the skin of wild-type mice. EPPK (visualized in red) was expressed mainly in the upper layer of the epidermis (B and F) and it appeared to be colocalized predominantly with K10 in merged images (C and G). In EPPK $^{-/-}$ mice, K5 and K10 were expressed in the basal layers and suprabasal layers (D and H), respectively, as in wild-type mice. (Dashed lines indicate basal lamina and the solid line represents the surface of the stratum corneum.) Panel I shows immunostaining of suprabasal keratinocytes of a wild-type mouse with gold-conjugated antibodies against EPPK (15 nm) and against K10 (5 nm; arrowheads). EPPK appears to be located in close proximity to keratin filaments, which were immunostained with antibodies specific for K10. Bars = 10 μm in A–H or 200 nm in I.

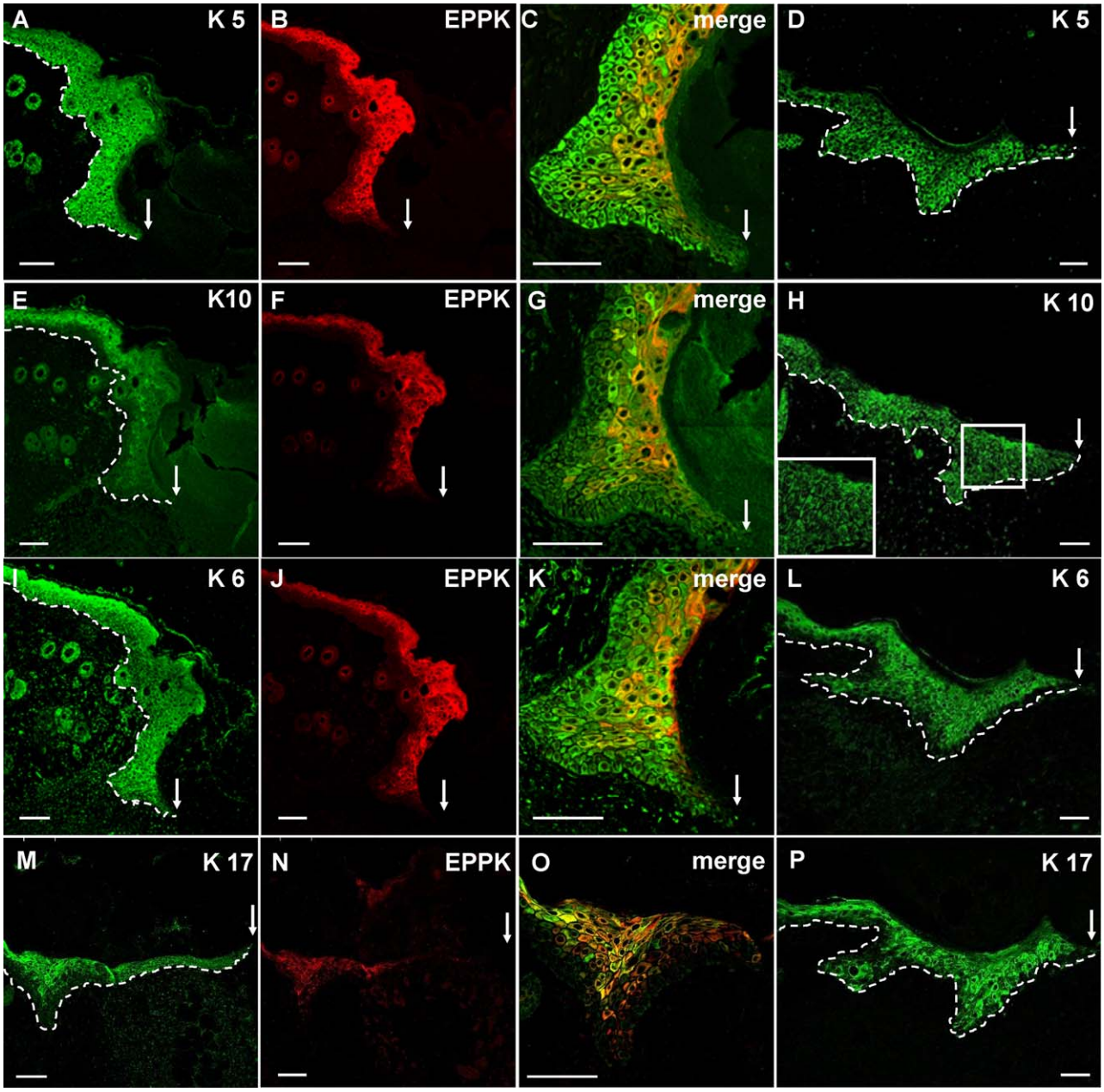

Fig. 2. Analysis by confocal laser scanning microscopy of wounds in wild-type (A–C, E–G, I–K, and M–O) and EPPK$^{-/-}$ (D, H, L and P) mice on day 4. K5 (visualized in green) was expressed not only in the basal keratinocytes but also in the hypertrophic epidermis around the wound edge and at the tip of the leading edge (A). K10 (E) and K6 (I) (visualized in green) were expressed mainly in suprabasal keratinocytes but also in basal keratinocytes. K17 (M) (visualized in green) was expressed mainly in the suprabasal region of the proliferating epidermis. EPPK (visualized in red) was expressed in the proliferating epidermis and, especially in the upper-middle layers of the wound edge (B, F, J and N). EPPK was colocalized predominantly with K17 in the keratinocytes at the wound edge (O). EPPK was not expressed at the tip of the leading edge (arrows) during wound closure. The merged images, which are shown at 2× magnification, revealed that larger epidermal cells that coexpressed K5, K10, K6 and K17 (C, G, K and O). In wounds of EPPK$^{-/-}$ mice on day 4, the expression of keratins resembled that in wild-type mice (D, H, L and P). Dashed lines indicate basal lamina and arrows represents at the tip of the leading edges. The inset in H shows white rectangle at 2× magnification. Bars = 50 μm.

contained relatively thick bundles of keratin around the nuclei (Fig. 3B and D). There were thick and straight keratin bridges between desmosomes and curved bundles of keratin around the nuclei (Fig. 3C and E). The intercellular spaces were wide but of relatively constant width near the basal layer.

In EPPK$^{-/-}$ mice, 4 days after wounding, the cytoplasm stained less strongly than in wild-type mice because the keratin fibers were so thin that they were not clearly visible at low magnification (Fig. 3H and J). At higher magnification, no thick keratin filaments were visible around the nuclei of keratinocytes near the basal layer at the wound's edge (Fig. 3I). There were very few straight keratin bridges between desmosomes and few curved keratin fibers around nuclei. These observations suggested that the absence of EPPK had decreased the formation of thick bundles of keratin (Fig. 3K). Near the basal layer, intercellular spaces were so irregular and so much wider than those in wild-type mice that many more red blood cells were able to enter these spaces.

While the keratin fibers connected to desmosomes in wild-type mice were thick and had coalesced, those in EPPK$^{-/-}$ mice were thin and individual fibers could be distinguished (Fig. 3F and L).

In the keratinocytes at the wound's edge in wild-type mice, 6 days after wounding, the aggregation of keratins was more extensive than on day 4 (Fig. 4C and E). Bundles of keratin appeared to extend across desmosomes between neighboring cells

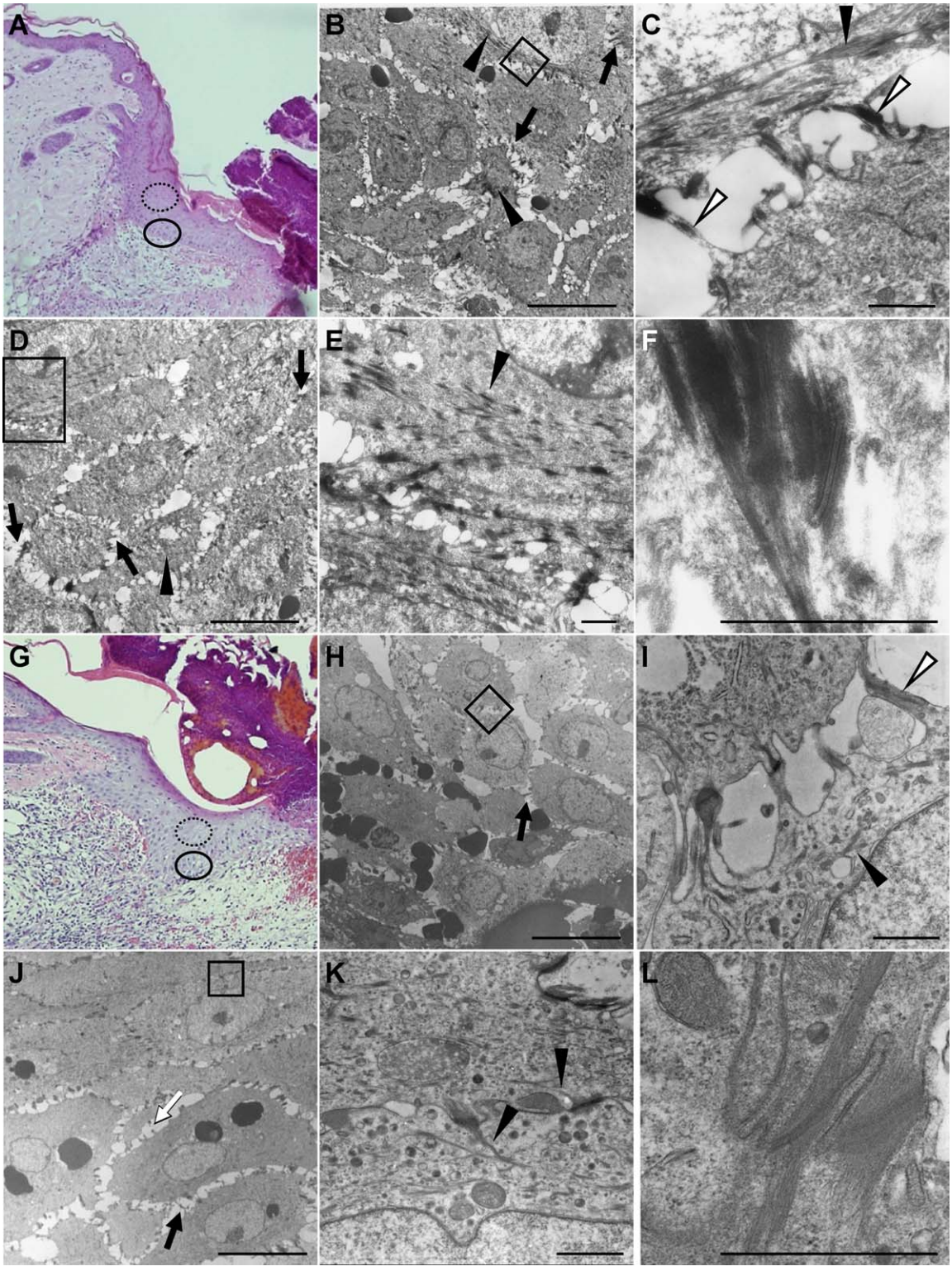

Fig. 3. Analysis of electron microscopy of wounds of wild-type (A–F) and EPPK$^{-/-}$ (G–L) mice on day 4. Light micrographs (A and G) are shown for reference and two sites, around the basal layer (solid ellipse) and the suprabasal layer (dashed ellipse), were examined by electron microscopy. Panels B, C, H and I are electron micrographs around the basal layer and panels D–E and J–K are those of the suprabasal layer. The areas in panels B, D, H and J enclosed by rectangles were magnified to yield panels C, E, I and K respectively. In wild-type mice, the cytoplasm was strongly stained and contained relatively thick bundles of keratin (black arrowheads) around nuclei in keratinocytes near the basal (B and C) and in the suprabasal (D and E) layer, as seen both at lower and higher magnification. The keratin fibers were connected to desmosomes (white arrowheads in C). The intercellular spaces around wild-type keratinocytes were relatively regular and cells were connected via a number of junctions that included desmosomes (arrows in B and D). The keratin fibers connected to desmosomes in wild-type mice were thick and had coalesced (F). In EPPK$^{-/-}$ mice, at lower magnification, the cytoplasm was only weakly stained because the keratin fibers were so thin that they were not clearly visible in the cytoplasm of both keratinocytes near the basal (H) and in the suprabasal (J) layer. At higher magnification (I), only thin keratin filaments were around nucleus (dark arrowhead) and no thick keratin filaments were connected to desmosomes (white arrowhead) around the basal layer at the wound edge. In the suprabasal layer, only thin keratin fibers (black arrowheads) were connected to desmosomes (K). Intracellular spaces between EPPK$^{-/-}$ keratinocytes were much wider than in the wild-type and the cells were connected via fewer junctions that included desmosomes (arrows in H and J). Some truncated junctions (white arrow) were also observed (J). The keratin fibers connected to desmosomes in EPPK$^{-/-}$ mice were thin and individual fibers were clearly visible (L). A and G were stained with hematoxylin and eosin. Bars = 10 μm in B, D, H and J or 1 μm in C, E, F, I, K and L.

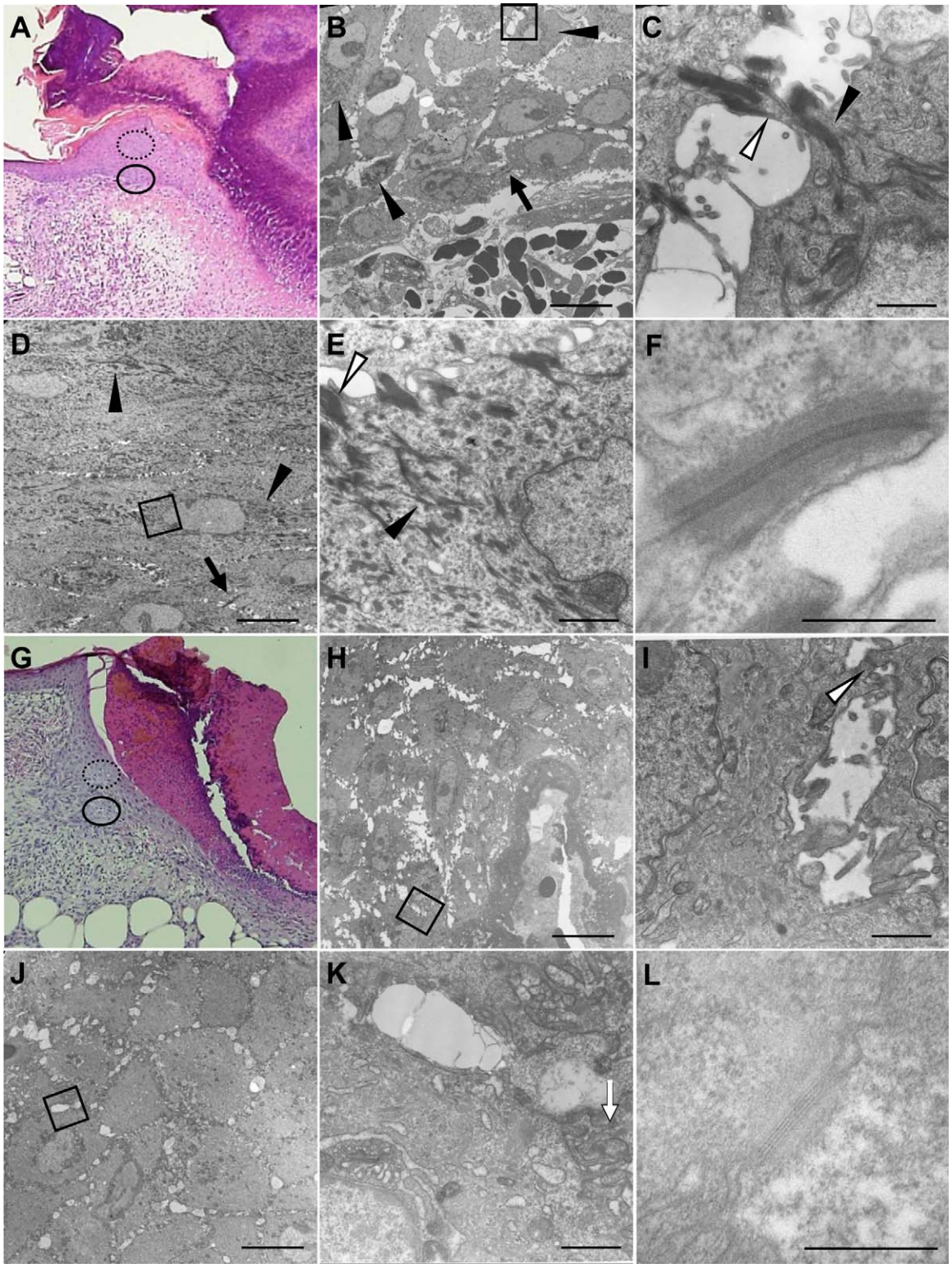

Fig. 4. Analysis by electron microscopy of wounds in wild-type (A–F) and EPPK$^{-/-}$ (G–L) mice on day 6. The regions around the basal layer (solid ellipse) and the suprabasal layer (dashed ellipse) on light micrographs (A and G) provided for reference, were examined by electron microscopy. Panels B, C, H and I are electron micrographs around the basal layer and panels D, E, J and K are those of the suprabasal layer. The areas in panels B, D, H and J enclosed by rectangle were magnified to yield images in panels C, E, I and K respectively. Although, on day 6, the difference in terms of the distribution of keratin between wild-type and EPPK$^{-/-}$ mice was essentially the same as on day 4, the aggregates of keratins in wild-type keratinocytes were denser than those on day 4. Thick bundles of keratin (black arrowheads) were seen around the nuclei in wild-type keratinocytes (B and D). Higher magnification revealed that these thick bundles of keratin (black arrowheads) were connected to desmosomes (white arrowheads in C and E). Intracellular spaces were quite regular (B), and keratins spanning desmosomes were also observed (arrows in B and D). In EPPK$^{-/-}$ mice, keratins were diffusely distributed throughout the entire cytoplasm (H and J) and there were some desmosomes and few keratin fibers around the desmosomes (white arrowhead in I). Desmosomes were underdeveloped (white arrow in K). Intracellular spaces were irregular (H and J) compared to those between wild-type keratinocytes (B and D). Although keratin fibers around the desmosomes were electron dense in wild-type mice (F), those were not electron dense in EPPK $^{-/-}$ mice (L). A and G were stained with hematoxylin and eosin. Bars = 10 μm in B, D, H and J or 1 μm in C, E, I and K or 500 nm in F and L.

(Fig. 4C). These observations suggested that keratinocytes might be under mechanical stress and subject to intracellular tension during wound healing. The intercellular spaces between basal cells were narrower than they had been on day 4 (Fig. 4B and D).

In the keratinocytes at the wound's edge in EPPK$^{-/-}$ mice, 6 days after wounding, keratin fibers remained faintly visible and no bundles of keratin were obvious near the desmosomes (Fig. 4H–K). At lower magnification, intracellular bridges appeared irregular and

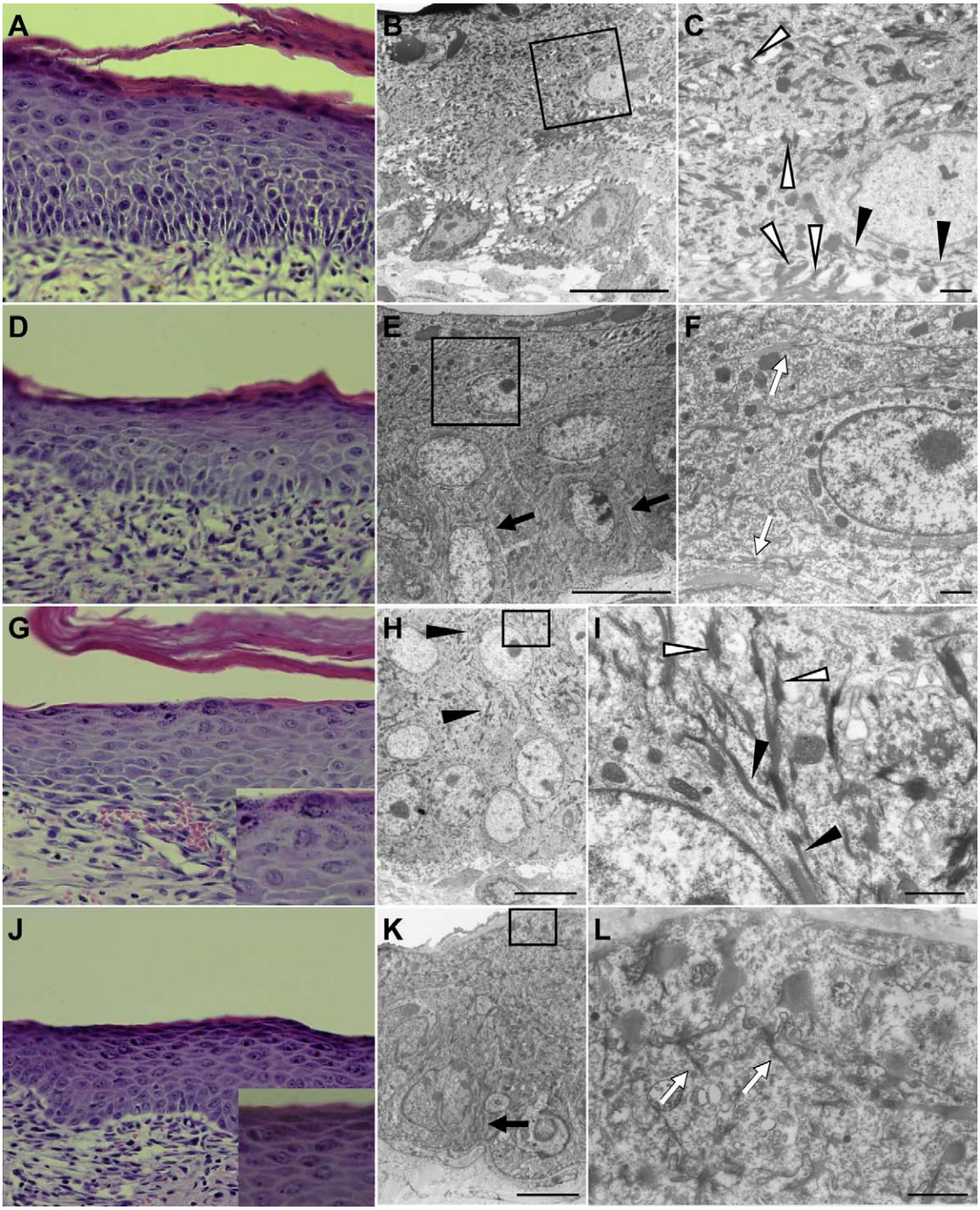

Fig. 5. Analysis by electron microscopy of wounds on day 8 (A–F), 10 (G–L) in wild-type (A–C and G–I) and EPPK$^{-/-}$ (D–F and J–L) mice. Light micrographs (A, D, G and J) are shown for reference. The areas enclosed by rectangle in panels B, E, H and K were magnified to yield panels C, F, I and L respectively. On day 8, wounds on the backs of both wild-type (A) and EPPK$^{-/-}$ (D) mice had closed. Wounds on wild-type mice closed more slowly than those on EPPK$^{-/-}$ mice, and intracellular spaces were more apparent around the basal layer of wild-type epidermis (B) than around that of EPPK$^{-/-}$ epidermis (E). Thin and less aggregated keratin fibers (black arrowhead) were evident around nuclei from the basal keratinocytes to the upper spinous keratinocytes (C) and some of these keratin bundles were connected to desmosomes (white arrowheads in C). In EPPK$^{-/-}$ mice, relatively thin keratin fibers (arrows) were visible in basal keratinocytes (E) and similar relatively thin keratin fibers (white arrows) were observed in the upper spinous keratinocytes (F). On day 10, few intracellular spaces were observed around the basal layer of wild-type epidermis (H). Keratin fibers were thin (black arrowheads in H and I) in the spinous layer and these fibers were connected to desmosomes (white arrowheads in I). In EPPK$^{-/-}$ mice, relatively thin keratin fibers were observed in basal cells (arrow in K) and they were connected to desmosomes (white arrows in L), and these fibers were still thinner than those in wild-type mice. Insets in G and J show granular layer at higher magnification. A, D, G and J were stained with hematoxylin and eosin. Bars = 10 μm in B, E, H and K or 1 μm in C, F, I and L.

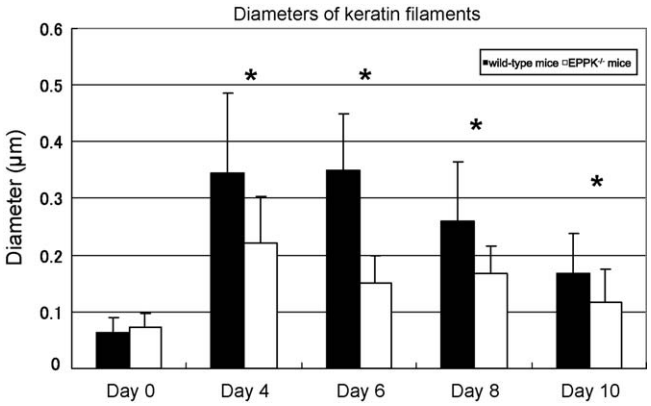

Fig. 6. The diameters of keratin filaments in keratinocytes from wild-type (black columns) and EPPK$^{-/-}$ (white columns) mice at various times after wounding. Diameters of keratin filaments were measured on electron micrographs. The keratin filaments in EPPK$^{-/-}$ mice were thinner than those in wild-type mice throughout wound healing. Values of each column are means ± SD of results from 250 measurements of fibers from 6 individual mice. Values that are significantly different on respective days are indicated by an asterisk ($P < 0.01$; Student's *t*-test).

desmosomes were underdeveloped (Fig. 4K). The widths of intercellular spaces between basal cells were irregular (Fig. 4H and J).

Although the keratin fibers adjacent to the desmosome were electron dense in wild-type mice (Fig. 4F), those were not electron dense in EPPK$^{-/-}$ mice (Fig. 4L).

Eight days after wounding, the entire wound of each wild-type mouse was covered with 9 or 10 layers of keratinocytes (Fig. 5A). Keratin fibers around nuclei had become more or less aggregated than they had been 6 days after wounding (Fig. 5B and C). The wounds of EPPK$^{-/-}$ mice were covered with 6–8 layers of keratinocytes at this time, but keratin fibers were still only faintly visible, especially near the corneal layers (Fig. 5E and F). The keratin fibers in the basal cells of EPPK$^{-/-}$ mice were thinner than those of wild-type mice (Fig. 5B and E). There were minimal intercellular spaces around the basal cells in EPPK$^{-/-}$ mice, as compared to those of wild-type mice (Fig. 5B and E). These observations suggested that wound healing had proceeded more rapidly in EPPK$^{-/-}$ mice than in wild-type mice, confirming previously reported results [6].

The thickness of the epidermis at the site of the wound in each wild-type mouse resembled that in EPPK$^{-/-}$ mice 10 days after wounding. However, granular layers were thicker in the mutant mice (Fig. 5G and J). In the keratinocytes of wild-type mice, 10 days after wounding, the keratin fibers around nuclei were thin (Fig. 5H and I). In the keratinocytes of EPPK$^{-/-}$ mice, at this time, keratin fibers were slightly thinner than on day 8 and they extended across desmosomes (Fig. 5K and L). The thickness of the epidermis of EPPK$^{-/-}$ mice decreased to 4–5 layers of cells on day 15 after wounding, when the thickness of hypertrophic granular layers had decreased. There were no obvious differences between the regenerated epidermis of wild-type and EPPK$^{-/-}$ mice 30 days after wounding (data not shown).

3.4. The diameters of keratin bundles in wild-type mice were greater than those in EPPK$^{-/-}$ mice

We compared the diameters of keratin bundles in the proliferating keratinocytes at wound edges in wild-type and EPPK$^{-/-}$ mice as wounds healed. The diameters of keratin bundles in wild-type mice were significantly greater ($P < 0.01$, student's *t*-test) than those of EPPK$^{-/-}$ mice throughout wound healing, as shown in Fig. 6.

3.5. The colocalization of K5, K6, K10 and EPPK

Electron microscopy after immunostaining of K5, K6, K10 and EPPK revealed that, in wild-type mice, keratin bundles in keratinocytes 4 days after wounding contained K5, K6 and K10. Moreover, EPPK was colocalized with K5, K6 and K10 during wound healing (Fig. 7A–C). These observations indicated that EPPK associated not only with K1/10 but also with K5/K14 and K6/K16 or K17 during wound healing.

4. Discussion

During wound closure, the expression and organization of the various keratins that we examined changed dramatically. Confocal laser scanning microscopy revealed similar patterns of keratin expression in EPPK$^{-/-}$ mice to those in wild-type mice. Thus, the absence of EPPK did not affect the expression of keratins during re-epithelialization. However, electron microscopy revealed considerable differences in terms of the distribution and aggregation of keratins between wild-type and EPPK $^{-/-}$ mice.

Four days after wounding, keratinocytes increased in size at the wound edge. In the cytoplasm of these proliferating keratinocytes in wild-type mice, keratins surrounded the nucleus and radiated

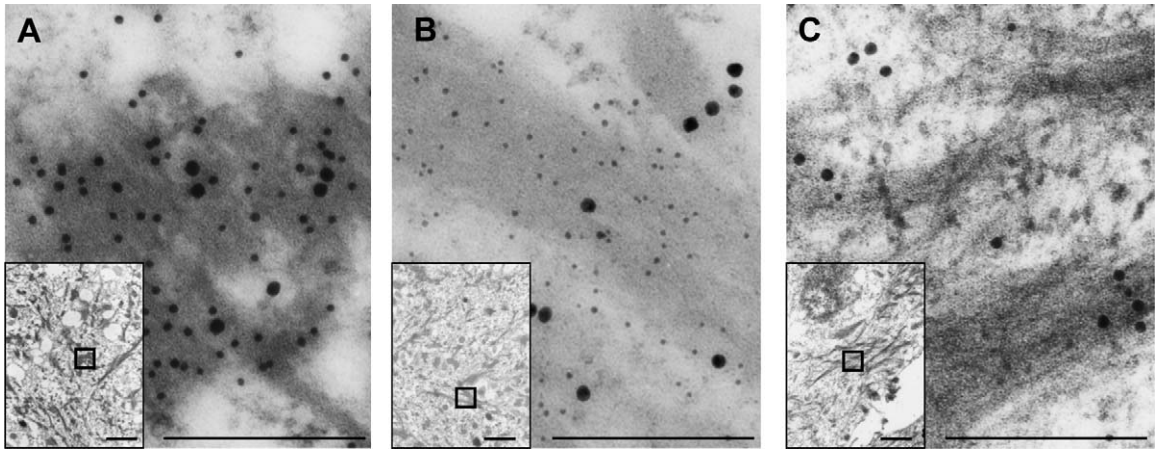

Fig. 7. Localization of immunogold-stained EPPK, K5, K6, and K10 in proliferating keratinocytes at wound edges on day 4 in wild-type mice. The areas enclosed by squares in the lower-left insets were magnified to generate the large photographs (bars in the insets represent 1 μm; bars in the magnified photographs represent 200 nm). EPPK (15-nm gold particle) was located in close proximity to K5 (10-nm gold particle in A), K6 (5-nm gold particles in B) and K10 (10-nm gold particles in C).

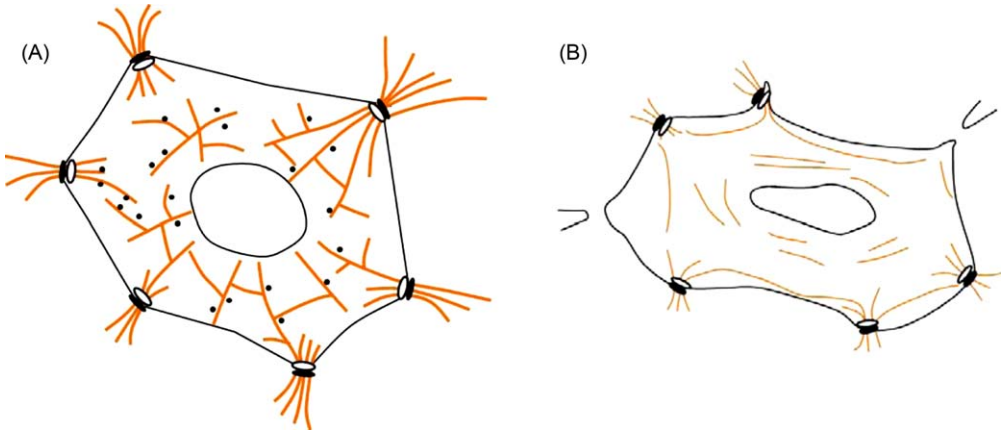

Fig. 8. Schematic models of molecular links between EPPK (black dots), keratins and desmoplakin (white ellipse) in the proliferating keratinocytes. Black ellipses represent desmosomes. Although keratin fibers are thick in wild-type mice (A), those are thin in EPPK $^{-/-}$ mice (B).

into the desmosomes. As the keratin bundles became thicker, they resembled a network. From day 8 to day 10, these bundles gradually became thinner.

By contrast, in EPPK$^{-/-}$ mice, keratin fibers were thin throughout re-epithelialization, suggesting that EPPK might accelerate the bundling of keratin filaments during wound healing. The formation of bundles of intermediate filaments results in increased elasticity, and greater elasticity increases resistance to shearing forces [7] (Fig. 8A and B).

At wound edges in wild-type mice, EPPK was expressed in proliferating keratinocytes; in EPPK $^{-/-}$ mice, there were fewer proliferating keratinocytes and, of course, no EPPK was produced [6]. EPPK was colocalized predominantly with K17 in the keratinocytes at wound edges, in wild-type mice (Fig. 2O) and we determined the dimensions of proliferating keratinocytes around wound edges using NIH imaging software to analyze electron micrographs after immunostaining of K17. The dimensions of keratinocytes from wild-type and EPPK$^{-/-}$ mice differed significantly only on day 6, with the former being larger than the latter. There were no significant differences between respective sizes of wound-edge cells in wild-type and mutant mice on day 4 and day 8. The smaller size of keratinocytes in EPPK$^{-/-}$ mice on day 6 suggests that keratinocytes without densely bundled intermediate filaments are subjected to shrinkage due to mechanical stress.

After double immunostaining, electron microscopy revealed that EPPK was colocalized with K10 in normal cornifying epithelium, and with K5, K6 and K10 in the proliferating keratinocytes at wound edges. The binding of EPPK to K5/K14 has been reported previously [3,5]. The association of EPPK with other keratins, as suggested by our observations, remains to be confirmed by analyses *in vitro*. In the normal epidermis, K1 and K10 are associated with the marked propensity of 10-nm keratin filaments to aggregate laterally and form dense bundles [8]. Moreover, in activated keratinocytes, K6/K16 and K6/K17 form bundled filaments [9,10]. It seems likely that EPPK contributes to this bundling of keratin fibers.

It is unclear why keratinocytes migrate more rapidly in EPPK$^{-/-}$ mice than in wild-type mice. However, the less extensive bundling of keratins, as finer fibers, that is associated with the absence of EPPK might be related to the enhanced migration observed in ex vivo skin explant cultures of K6-null keratinocytes [11]. The molecular events involved in the association with keratins remain to be clarified. They might be linked to elevated states of phosphorylation of Erk kinase as observed in plectin-deficient mouse keratinocytes [12] or to increased levels of total and tyrosine-phosphorylated p120 catenin, as observed in K6-deficient mouse keratinocytes [13,14]. At the moment we could not find the interaction between EPPK and actin or microtubules or related linkers, which are more closely related to cell migration.

Plectin-deficient mouse keratinocytes migrate more rapidly than wild-type cells, and the former contain networks of massively bundled keratin with large spaces between the bundles *in vitro* [12]. Although faster migration of keratinocytes is also a feature of EPPK deficiency, the keratin bundles have exactly the opposite features. The difference is very likely due to the different functions of EPPK and plectin: EPPK might contribute to the bundling of intermediate filaments while plectin might increase their stiffness by introducing orthogonal cross-links between filaments. Periplakin is another member of the plakin family, which, unlike EPPK, has no PRD repeats at its carboxyl terminus, but contains specific amino-terminal and rod domains. "Knock-down" of periplakin by siRNA inhibited the organization of keratin and impaired the migration of epithelial cells [15]. Thus, different cross-linking proteins have clearly different functions.

The impaired bundling of keratin filaments in proliferating keratinocytes at wound edges in EPPK$^{-/-}$ mice suggests that EPPK might accelerate the lateral organization of keratin filaments when hypertrophy of keratinocytes is required for wound healing. This is the first report, to our knowledge, that EPPK affects the architecture of intermediate filaments *in vivo*.

Appendix A. Supplementary data

Supplementary data associated with this article can be found, in the online version, at doi:10.1016/j.jdermsci.2010.08.011.

References

[1] Fujiwara S, Takeo N, Otani Y, Parry DA, Kunimatsu M, Lu R, et al. Epiplakin, a novel member of the plakin family originally identified as a 450-kDa human epidermal autoantigen. Structure and tissue localization. J Biol Chem 2001;276:13340–7.
[2] Spazierer D, Fuchs P, Pröll V, Janda L, Oehler S, Fischer I, et al. Epiplakin gene analysis in mouse reveals a single exon encoding a 725-kDa protein with expression restricted to epithelial tissues. J Biol Chem 2003;278:31657–66.
[3] Jang SI, Kalinin A, Takahashi K, Marekov LN, Steinert PM. Characterization of human epiplakin: RNAi-mediated epiplakin depletion leads to the disruption of keratin and vimentin IF networks. J Cell Sci 2005;118:781–93.
[4] Wang W, Sumiyoshi H, Yoshioka H, Fujiwara S. Interactions between epiplakin and intermediate filaments. J Dermatol 2006;33:518–27.
[5] Spazierer D, Raberger J, Gross K, Fuchs P, Wiche G. Stress-induced recruitment of epiplakin to keratin networks increases their resistance to hyperphosphorylation-induced disruption. J Cell Sci 2008;121:825–33.
[6] Goto M, Sumiyoshi H, Sakai T, Fässler R, Ohashi S, Adachi E, et al. Elimination of epiplakin by gene targeting results in acceleration of keratinocyte migration in mice. Mol Cell Biol 2006;26:548–58.
[7] Coulombe PA, Omary MB. 'Hard' and 'soft' principles defining the structure, function and regulation of keratin intermediate filaments. Curr Opin Cell Biol 2002;14:110–22.

[8] Coulombe PA, Kopan R, Fuchs E. Expression of keratin K14 in the epidermis and hair follicle: insights into complex programs of differentiation. J Cell Biol 1989;109:2295–312.
[9] Paladini RD, Takahashi K, Bravo NS, Coulombe PA. Onset of re-epithelialization after skin injury correlates with a reorganization of keratin filaments in wound edge keratinocytes: defining a potential role for keratin 16. J Cell Biol 1996;132:381–97.
[10] Paladini RD, Coulombe PA. Directed expression of keratin 16 to the progenitor basal cells of transgenic mouse skin delays skin maturation. J Cell Biol 1998;142:1035–51.
[11] Wong P, Coulombe PA. Loss of keratin 6 (K6) proteins reveals a function for intermediate filaments during wound repair. J Cell Biol 2003;163:327–37.
[12] Osmanagic-Myers S, Gregor M, Walko G, Burgstaller G, Reipert S, Wiche G. Plectin-controlled keratin cytoarchitecture affects MAP kinases involved in cellular stress response and migration. J Cell Biol 2006;174:557–68.
[13] Cozzolino M, Stagni V, Spinardi L, Campioni N, Fiorentini C, Salvati E, et al. p120 catenin is required for growth factor-dependent cell motility and scattering in epithelial cells. Mol Biol Cell 2003;14:1964–77.
[14] Coulombe PA, Wong P. Cytoplasmic intermediate filaments revealed as dynamic and multipurpose scaffolds. Nat Cell Biol 2004;6:699–706.
[15] Boczonadi V, McInroy L, Määttä A. Cytolinker cross-talk: periplakin N-terminus interacts with plectin to regulate keratin organisation and epithelial migration. Exp Cell Res 2007;313:3579–91.